Forecasting Liquefaction Hazard from Seattle Fault Zone Earthquakes: Impacts on a Major Metropolitan Area

Ryan A. Rasanen[1]

Abstract:

The Seattle Fault Zone (SFZ), a 70-km-long thrust fault system beneath Seattle, Washington, poses a significant seismic hazard to the Puget Sound region due to its proximity to dense urban infrastructure. While other coseismic hazards, such as tsunamis, landslides, and structural damage, have been forecasted for SFZ earthquakes and garnered considerable attention, soil liquefaction—despite its potential for widespread disruption—remains understudied. This study forecasts the spatial distribution of liquefaction and its potential impacts on civil infrastructure from three M_w7.2 SFZ earthquake scenarios. Leveraging an ensemble of 18 popular cone-penetration-test based liquefaction models at 268 newly compiled study sites, 14,472 individual high-quality liquefaction predictions are made across the Puget Sound region. Results reveal that severe liquefaction is expected in Seattle and nearby suburbs, particularly within 20 km of the fault along the Interstate-5 corridor, where fill and alluvial soils are prevalent. Comparisons to the 2001 M_w6.8 Nisqually earthquake and a potential M_w9.0 Cascadia Subduction Zone rupture indicate that SFZ earthquakes are expected to produce more severe liquefaction effects near Seattle due to their closer proximity and greater shaking intensities at short-to-moderate periods. Additionally, liquefaction-induced damage to shallow foundations is predicted to be widespread in Seattle and its suburbs but more limited in areas farther from the fault. These findings provide insights for government agencies and stakeholders to better prepare for future SFZ ruptures.

Keywords: Soil Liquefaction; Seattle Fault Zone; Earthquake Engineering; Liquefaction Hazard; Natural Hazard; Ground Failure

1.0 Introduction and Motivation

The Seattle Fault Zone (SFZ), a 70-km-long thrust fault system, stretches east-west beneath the city of Seattle, Washington, and is considered the most hazardous crustal fault in the U.S. Pacific Northwest due to its proximity to a major urban center (Liberty and Pratt 2008). The SFZ is capable of producing earthquakes in the magnitude range of M_w7.0–7.5 (e.g., ten Brink et al. 2006; Nelson et al. 2014; Styron and Sherrod 2021) and evidence of surface deformation suggests that moderate-to-large earthquakes (~Mw 5.5–7.5) may occur every few hundred years during active phases lasting approximately 1,000–2,000 years,

[1] Dept. of Civil & Environmental Eng., University of North Carolina at Charlotte, Charlotte, NC, USA.
e-mail: rrasanen@charlotte.edu
ORCiD: https://orcid.org/0000-0002-3151-187X

followed by quiescent periods lasting several thousand years or more (Nelson et al. 2014). The most recent large rupture, which occurred between 900–930 CE (Bucknam et al. 1992; Atwater, 1999; Sherrod 2001), caused significant geological effects such as liquefaction (Atwater 1999; Atwater personal communication 2020; Bourgeois and Johnson 2001; Martin and Bourgeois 2012; Whistler et al. 2002), tsunamis (Atwater 1999; Atwater and Moore 1992; Bourgeois and Johnson 2001), and landslides (Jacoby et al. 1992; Karlin et al. 2004; Ludwin et al. 2005; Schuster et al. 1992). Black et al. (2023) further constrained this SFZ rupture to a 6-month period between 923 and 924 CE using dendrochronological dating methods and suggested it may have been a multi-fault M_w7.8 rupture involving simultaneous rupture of the SFZ and Saddle Mountain fault.

In anticipation of future SFZ earthquakes, several hazards have been forecasted, including tsunamis (Chamberlin and Arcas 2015; Dolcimascolo et al. 2022; Koshimura et al. 2006; Martin 2012; Raulerson 2021;), landslides (Allstadt et al. 2013; Grant (2017); Herzig et al. 2024), and shaking-related structural damage (Stewart 2005). These hazards have garnered considerable attention (e.g., Dolcimascolo et al. 2022), and decisions on public safety have directly stemmed from them. However, one critical hazard from a SFZ rupture—soil liquefaction—has received comparatively less attention, despite its potential to cause extensive economic and infrastructural damage (e.g., Huang and Yu 2013). Liquefaction, a phenomenon where loose saturated sand-like soils lose strength due to earthquake shaking, has historically caused severe impacts, as exemplified by the Canterbury, New Zealand earthquakes, where liquefaction alone accounted for approximately $10 billion in damages (Parker and Steenkamp, 2012). In Seattle and the surrounding Puget Sound region, the potential impacts of liquefaction are particularly concerning given the dense urban infrastructure, including buildings, bridges, port structures, roads, levees, and lifelines. For example, Stewart (2005) estimated that a scenario M_w6.7 SFZ earthquake could result in 9,700 destroyed buildings, 154,500 moderately or severely damaged buildings, 24,200 injuries, and 1,660 fatalities, with liquefaction contributing significantly to these impacts. While these estimates rely on numerous simplifying assumptions and warrant further investigation, they underscore the potentially staggering impact of liquefaction from a SFZ rupture.

Instances of liquefaction have been documented in the Puget Sound region during the region's recent large historical earthquakes, such as the 1949 M_w7.1 Olympia earthquake and the 1965 M_w6.5 Seattle-Tacoma earthquake (Chleborad and Schuster 1990). While these events caused only moderate damage in Seattle due to relatively low peak ground accelerations (*PGA*s) of approximately 0.10 g (Rogers et al. 1998), they serve as a reminder of the hazard's potential. Grant (1986) estimated that 25–50% of the total damage from these earthquakes could be attributed to ground failures such as liquefaction. More recently, the 2001 M_w6.8 Nisqually earthquake also damaged infrastructure throughout the Puget Sound region causing $2 to 4 billion in damage (Creager et al. 2001). Despite these past earthquakes, the damage potential in Seattle is

expected to be far greater in a large SFZ event compared to any other seismic source in the region due to the shallow depth of the fault and its close proximity to the city, leading to significantly higher shaking intensities, particularly for short-to-moderate periods.

Despite its importance, the only prior attempt to forecast the spatial distribution of liquefaction in an SFZ rupture is Stewart's (2005) study, which employed the HAZUS geospatial modeling approach (e.g., FEMA 2019). This method assigns broad hazard classifications (e.g., "low" to "high") to geologic units based on several simplifying assumptions. While useful for providing a first-order approximation, geospatial models like HAZUS, which infer soil traits from geologic maps, are inherently less reliable than mechanistic liquefaction models that use detailed below ground geotechnical data. As a result, neither the expected spatial distribution of liquefaction in a large SFZ event nor its damage potential for infrastructure is currently understood with confidence.

Mechanistic models, first developed in the 1970s (e.g., Seed and Idriss, 1971), have significantly advanced the prediction of liquefaction occurrence and damage potential using geotechnical test data. These state-of-practice models, refined over decades with expanded datasets (e.g., Geyin et al. 2021), achieve global prediction efficiencies of ~75–85% (e.g., Geyin and Maurer 2020a). For instance, during the Nisqually earthquake, a popular ensemble of these models demonstrated ~90% efficiency in predicting liquefaction occurrence (Rasanen et al., 2023a). Despite their proven reliability, no study has applied these mechanistic liquefaction models to predict the spatial distribution and damage potential of liquefaction in a large SFZ earthquake.

Accordingly, this study aims to fill this critical knowledge gap by forecasting the spatial distribution of liquefaction and its potential impacts on civil infrastructure during a large SFZ event using state-of-practice liquefaction models. This study first introduces the expected ground motions from three M_w7.2 SFZ earthquake scenarios and the geotechnical data used. It then presents the liquefaction modeling methodology followed by a discussion of the results with comparisons to past earthquakes. Lastly, the conclusions are presented. This research provides valuable insights to aid government agencies and stakeholders in preparing for and mitigating the risk of liquefaction posed by future SFZ earthquakes.

2.0 Data and Methodology

2.1 Seattle Fault Zone Scenarios

The Building Seismic Safety Council 2014 (BSSC2014) Event Set (Thompson et al. 2016) includes rupture scenarios of characteristics earthquakes on all known active faults in the United States as included in the 2014 version of the USGS national seismic hazard maps (Petersen et al. 2014). The ground motion intensity measures (e.g., *PGA*) in this catalog were computed using a weighted combination of ground motion models for reference rock conditions that are consistent with the 2014 USGS national seismic hazard maps

(Petersen et al. 2014). To account for local soil conditions, the BSSC2014 scenarios used the time averaged shear wave velocity over the top 30 meters (V_{s30}) to compute empirical site amplification factors (V_{s30}-based site amplification). Each of the ground motions models used its own site response model (e.g., Chiou and Youngs 2014) or one developed for particular ground motion models (e.g., Seyhan and Stewart 2014). The input V_{s30} values are a combination of a global model estimated from topographic slope (Wald and Allen 2007) and regional models that are available at the USGS Global V_{s30} GitHub repository (Worden and Heath, 2019). As part of the BSSC2014 scenario catalog, three SFZ zone earthquake scenarios were modelled—the northern, middle, and southern scenarios. Each of the three SFZ scenarios were modelled as M_w7.2 ruptures along a thrust fault at 9 km depth, but with varying locations and lengths (Petersen et al. 2008). Therefore, the shaking produced between the scenarios differs, especially in the near-field. The ground motion estimates for each of the scenarios include site-adjusted mean and standard deviation values for multiple intensity measures (e.g., *PGA*). In addition to ground motions estimates derived from ground motion models, physics-based ground motion simulations have more recently been developed for the SFZ. Stone et al. (2022) produced 20 physics-based simulations of M_w6.5-7.0 SFZ earthquakes using a variety of slip distributions and hypocenter locations. While the Stone et al. (2022) simulations potentially offer improved estimates of ground shaking at many frequencies, there are drawbacks for using them to predict regional liquefaction. First, the spatial extent of the Stone et al. (2022) simulations is limited to ~40 km from Seattle and thus does not cover the extent at which liquefaction can occur during a SFZ earthquake. Second, the SFZ simulations are modeled up to a frequency of 3 Hz, whereas *PGA* is the most efficient, sufficient, and commonly used intensity measure for predicting liquefaction (e.g., all state-of-art liquefaction response models use *PGA*) (Sideras, 2019). Therefore, to predict liquefaction across the region with the Stone et al. (2022) simulations, modification for use of high frequencies would be required in addition to a methodology to ensemble them with a GMM so they can be extended to sites across the region, both of which would add uncertainty to the predicted ground shaking. Therefore, while the Stone et al. (2022) simulations are an excellent source for many studies (e.g., Herzig et al. 2024), the SFZ BSSC2014 scenarios are used in this study to predict regional liquefaction impacts. Mean site-adjusted *PGA*s are shown for the three SFZ scenarios in Figure 1 along with 268 locations of subsurface geotechnical data as discussed in the following section. These mean *PGA* estimates, along with the corresponding standard deviation, are used to compute a probability density function (PDF) of *PGA* for use in liquefaction forecasts.

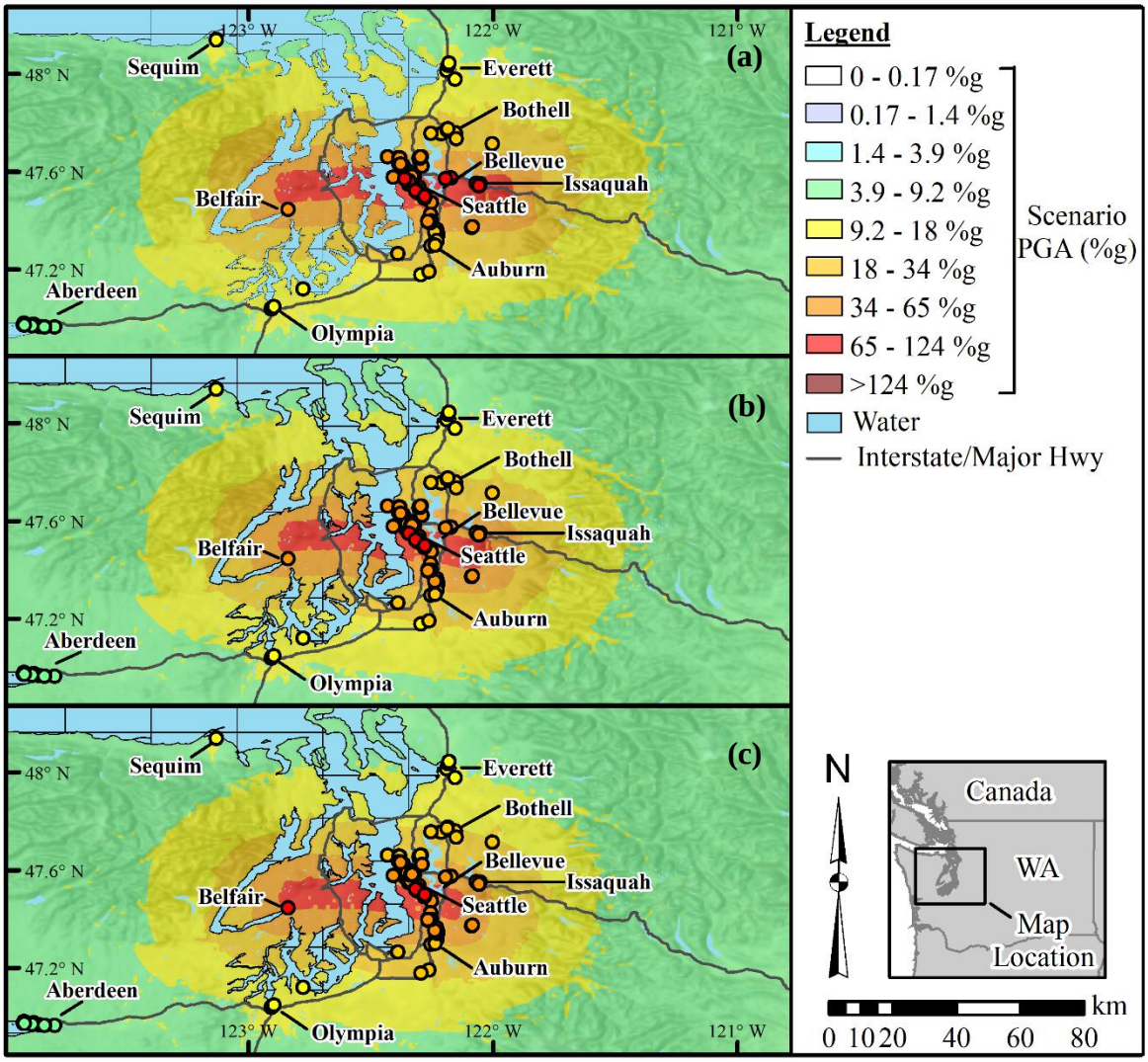

Fig. 1 Seattle fault shakemap of mapped *PGA* (%g) for (a) northern; (b) middle; and (c) southern scenarios with the locations of 268 study sites marked with circles. *PGA* = peak ground acceleration.

2.2 Subsurface Data and Methodology

To predict liquefaction response at 268 locations, a newly compiled dataset of CPT measurements and other geotechnical data was assembled from various sources, including Jeschke et al. (2019), Chin and Evans (2021), the Washington State Dept. of Transportation (WSDOT 2021), and Grant et al. (2024). The selected study sites were chosen based on SFZ scenarios predicting a *PGA* of at least 0.08 g at each site, which represents the minimum estimated *PGA* required to trigger liquefaction in even the most susceptible soils (de Magistris 2013). This dataset is made available in Rasanen et al. (2024; 2025) to support future research. Given the importance of saturation, groundwater depths were collected from the geotechnical reports that documented CPTs in addition to supplemental information from nearby borings, well logs, and test pits. In most cases, multiple groundwater depth measurements were available near each CPT location due to the

region's extensive subsurface exploration history. The locations of the 268 study sites are shown in Figure 1. They are spatially distributed but concentrated along the Interstate-5 (I-5) corridor from Olympia, WA to Everett, WA, including Seattle and many of its suburbs, and in coastal towns (e.g., Aberdeen, WA and Sequim, WA).

2.3 Liquefaction Modeling

Liquefaction triggering was predicted over the depths of each CPT profile using six established CPT-based methods: Robertson and Wride (1998), Architectural Institute of Japan (2001), Moss et al. (2006), Idriss and Boulanger (2008), Boulanger and Idriss (2016), and Green et al. (2019). Following findings from Geyin and Maurer (2021b) and Yost et al. (2021), no inversion filter was applied to account for thin-layer effects in the CPT data. Liquefaction susceptibility was assessed using soil behavior type index (I_c) (Robertson and Wride, 1998). To address the uncertain relationship between I_c and susceptibility, the Maurer et al. (2019) model was employed to estimate the probability of susceptibility, as defined by Boulanger and Idriss (2006), based on the measured I_c values. Since liquefaction occurring at depth may have minimal impact or fail to manifest at the ground surface, the results of the triggering analysis were used as inputs to three additional models to predict surficial manifestations of liquefaction (i.e., "ground failure"). These models—developed by Iwasaki et al. (1978), van Ballegooy et al. (2014), and Maurer et al. (2015)—do not explicitly predict infrastructure damage, but offer practical proxies of damage potential. Because more severe surface manifestations of liquefaction correlate with a higher likelihood of damage to near-surface infrastructure such as buildings, bridges, and roads, these models can provide insight into the potential severity of impacts. The combined use of six triggering models and three manifestation models resulted in 18 model combinations. Probabilistic predictions of surficial liquefaction manifestations were made for these 18 models using fragility functions developed by Geyin and Maurer (2021a). With this methodology, the probability of manifestation was computed using the total probability theorem as:

$$P(\text{Manifestation}) = \int_{PGA} \int_{I_c} P(\text{Manifestation}|PGA, I_c)\, f(I_c) f(PGA) \cdot \mathrm{d}I_c \cdot \mathrm{d}PGA \quad (1)$$

Where $f(I_c)$ is the probability density function of the I_c threshold for discriminating susceptibility (Maurer et al., 2019); $f(PGA)$ is the probability density function (PDF) computed from a weighted combination of ground motion models (GMMs) considering site response (Thompson et al. 2016); and $P(\text{Manifestation}|PGA, I_c)$ is the probability of surficial manifestation, which is conditioned on PGA and the susceptibility threshold I_c , among other inputs, and which is computed via the fragility functions of Geyin and Maurer (2021a). Rasanen et al. (2023a) evaluated the performance of these 18 models using 24 case histories from the 2001 Nisqually, WA, earthquake. While the predictive efficiencies of the models varied, the differences were generally not statistically significant when accounting for finite-sample

uncertainty. Therefore, in this study, predictions from all 18 models were combined using an ensemble approach with equal weighting.

3. Results and Discussion

3.1 Liquefaction Predictions

Using the data and methodology described above, the probability of surficial liquefaction manifestation was computed at 268 study sites for each of the 18 liquefaction models and the three SFZ ground-motion scenarios, resulting in 14,472 individual high-quality liquefaction predictions. The ensembled liquefaction probabilities, shown in Figure 2 for each SFZ scenario, indicate that the highest probabilities occur along the I-5 corridor near Seattle, WA. Given the sites available for study, probabilities exceeding 60% are in general predicted as far south as 30 km from Seattle, as far north as 20 km from Seattle, as far east as Issaquah, WA 25 km away from Seattle, and as far west as Belfair, WA 40 km away from Seattle. Also of note, are probabilities exceeding 60% in Olympia, WA (75 km from Seattle) for the southern SFZ scenario, and probabilities exceeding 20% as far Northwest as Sequim, WA for all scenarios. These predictions indicate that liquefaction could be widespread throughout the Puget Sound region, particularly near Seattle, posing substantial risks to densely populated areas, critical transportation networks, and infrastructure. Further away from the SFZ, the probabilities in Aberdeen, WA generally range from 1% to 5% and occasionally exceed 10% for all scenarios, while the probabilities in Everett, WA generally range from 10% to 20% where the northern scenario generally predicts ~2% higher probability on average. While the predicted probabilities are low in Aberdeen and Everett from a SFZ earthquake, other earthquakes such as a Cascadia Subduction Zone rupture (Rasanen et al. 2025) for Aberdeen, or a Whidbey Island crustal fault rupture for Everett, would almost certainly be more severe in those locations. Furthermore, this should not be taken to mean that liquefaction can only occur at the study sites investigated in this article. Rather, these are the locations where high-quality subsurface data is available to make predictions. It must be emphasized that while these predictions may generally extrapolate to areas surrounding each test site, liquefaction is a localized phenomenon and therefore nothing can be known with certainty at unsampled locations.

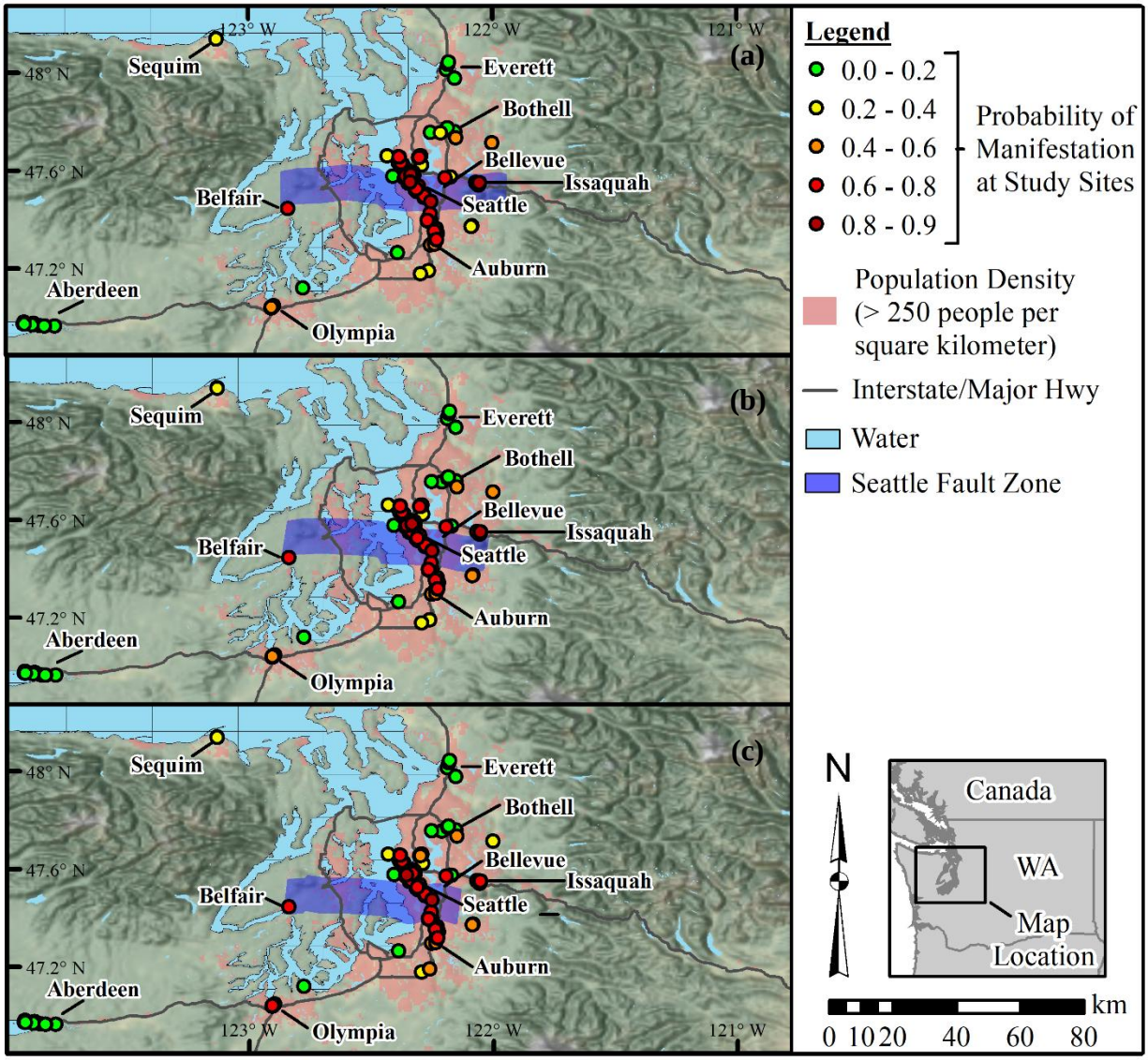

Fig. 2 Probability of liquefaction surface manifestation at 268 study sites considering the (a) northern; (b) middle; and (c) southern Seattle fault ground motion scenarios.

Due to the dense population and strong ground motions expected in the near-field for each scenario, Figure 3 provides a higher-resolution view of the predicted probability of liquefaction manifestation at study sites within a section of Seattle. Figure 3 provides results from the northern and southern SFZ scenarios, which among the three scenarios produce motions that differ the most. In this regard, the probability of liquefaction manifestations for the middle scenario are mapped in supplemental Figure S.4. Comparing liquefaction response between SFZ scenarios, the northern scenario predicts probabilities to be 5% larger on average than the southern scenario. This is the result of the northern SFZ scenario traversing beneath more of the Seattle study sites (rather than south of them) leading to a larger *PGA* prediction. In that regard, study sites in the near-field have larger probability differences between SFZ scenarios compared

to study sites further from the SFZ due to the larger differences in *PGA* in the near field. As an example, the probabilities in Seattle, Auburn, and Issaquah differ by ~5% between the northern and southern scenarios, but differ by ~2% in Everett and Olympia and trend to negligible differences further away in locations like Aberdeen. While perceptible differences in predictions of liquefaction exist between the SFZ scenarios, all scenarios predict significant liquefaction in Seattle with the average across the three scenarios exceeding 60% at 92 of the 140 study sites. The areas expected to be impacted most are the Greater Duwamish, Interbay, and University districts where a majority of the test data is located (see Figure 3). Of these districts, the Duwamish is expected to be most severely impacted by liquefaction with 70% of study sites having a probability > 60%, followed by Interbay (62%) and the University district (22%). Notably, these districts all have areas of extensive artificial fill and experienced liquefaction in the 1949, 1965, and/or 2001 earthquakes (e.g., Chleborad and Schuster 1990; Bray et al. 2001). To provide context for the computed probabilities, predictions of liquefaction for a SFZ earthquake are compared to those made for the 2001 Nisqually earthquake, which benefited from dense ground motion recordings and where observed liquefaction damage provides a benchmark for evaluating the relative severity of future events. Using the same modeling approach for the Nisqually event (Rasanen et al., 2023a), liquefaction probabilities in the Duwamish district for an SFZ scenario are approximately double those of the Nisqually event, while in Interbay and the University districts, probabilities are as much as 10 times higher. Therefore, the frequency and severity of liquefaction in the Duwamish district may be twice that experienced in 2001, where structures in the area were extensively damaged by liquefaction-induced foundation failure, with some foundations settling by as much as 4 feet. In total, 26 buildings in Seattle were red-tagged and 161 others yellow-tagged, the majority of which in the Duwamish district (Creager et al. 2001). For the Interbay and University districts, direct comparisons to the Nisqually event are more challenging due to minimal observed liquefaction and damage during the 2001 earthquake, a result of the northward attenuation of ground motions in that event. Nevertheless, given the proximity of these districts to the SFZ, significantly larger ground motions are expected compared to Nisqually, and the resulting liquefaction hazards would likely lead to far greater damage in these areas.

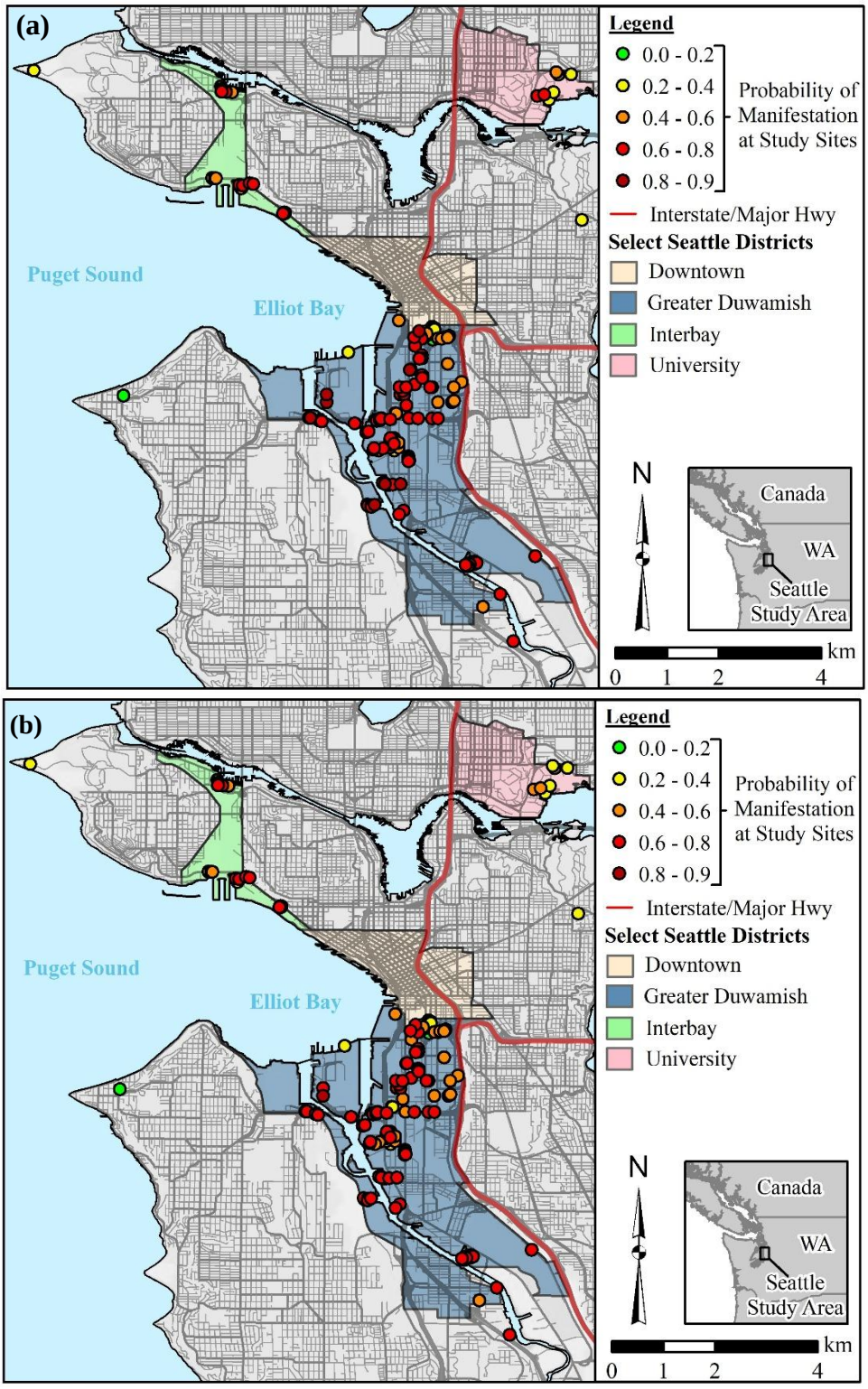

Fig. 3 Probability of liquefaction surface manifestation at study sites in Seattle, WA, considering the (a) northern; and (b) southern Seattle fault ground motion scenarios.

It should be noted in the context of Figures 2 and 3 that predictions cannot be extrapolated well beyond the study sites. In the University district, for instance, study sites near the University of Washington's athletic facilities are on land that was formerly beneath the surface of Lake Washington before its lowering around 1915, and where artificial fill is prevalent. In contrast, most of the University campus just to the west lies at higher elevations on glacial till, where the liquefaction hazard is expected to be very low. Similar statements could be made for the Interbay and Duwamish districts that also have reclaimed land. Importantly, this does not imply that liquefaction hazards are limited to these areas of Seattle. Artificial fill is widespread across the city, and as shown by historical and paleoliquefaction observations in the region (e.g., Rasanen et al. 2021), in addition to global earthquakes occurring each year, alluvium and other natural soil deposits can be equally susceptible to liquefaction. Furthermore, the predictions shown in Figure 3 are not representative of the entire city. Study sites are typically located where liquefiable soils are more likely to be found—such as areas with artificial fill or alluvium—rather than in locations with more resistant ground, like glacial till. Similar patterns can be observed in other municipalities, as CPTs are generally performed in soils that are sufficiently penetrable.

3.2 Comparisons of Seattle Fault Zone to M9 Cascadia Subduction Zone liquefaction

To provide additional details for towns outside Seattle, but still impacted by a SFZ rupture, their liquefaction predictions are discussed in more detail and then compared to liquefaction predictions from a Cascadia Subduction Zone (CSZ) rupture. Rasanen et al. (2025) predicted the regional probability of liquefaction manifestation from 30 M_w9.0 CSZ simulations. While there is no infrastructure damage to compare to like there is for the 2001 Nisqually earthquake, general comparisons between SFZ and CSZ predictions of liquefaction can be made. To that end, the SFZ predictions are compared to the median probabilities of the 30 M_w9.0 CSZ events.

Aberdeen, Washington: Probabilities in Aberdeen, WA for all scenarios generally range from 1% to 5% and occasionally exceed 10%. In general, the Southern Seattle fault scenario provides the highest predictions, although the differences are negligible between scenarios (~1%). The low probabilities in Aberdeen compared to other locations discussed are mainly due to Aberdeen's distance from the SFZ. The western extents of the three rupture scenarios are approximately 90 km from Aberdeen, allowing more distance for ground motions to attenuate. Therefore, the strength of ground shaking is much lower in Aberdeen (~0.08 g) compared to other near-fault locations like Seattle (~0.5-0.8 g) for the SFZ scenarios. Comparing to the expected liquefaction impacts from a CSZ rupture, Rasanen et al. (2025) predicted a median liquefaction response that ranged from 30-75% at the study sites in Aberdeen. Therefore, while the probability of liquefaction is low in Aberdeen for a SFZ rupture, other seismic sources such as the CSZ are likely to produce liquefaction.

Everett, Washington: Everett, WA is approximately 50 km north of the SFZ along I-5. The probabilities in Everett, WA generally range from 10 to 20%, where the north scenario generally predicts ~2% higher probability on average. Comparing with the expected liquefaction impacts from a CSZ rupture, Rasanen et al. (2025) found median liquefaction probabilities ranged from 20% to 47%. Therefore, although Everett is much closer to the SFZ than to the CSZ, the greater magnitude and longer shaking duration of a CSZ rupture results in higher probabilities of liquefaction manifestation in Everett.

Auburn, Washington: Auburn, WA is approximately 15 to 25 km south of the SFZ. The probabilities in Auburn generally range from 50% to 70%. The southern Seattle fault scenario provides the highest predictions for all sites in Auburn with probabilities 5% larger than the northern scenario on average. Thus, while the ground motions may appear similar in Figure 1 between scenarios, there are perceptible differences in liquefaction response owing to the differences in the ground motions at the site. Interestingly, CSZ median liquefaction probabilities are generally within ~1% to 2% of the middle Seattle fault scenario (i.e., between the southern and northern SF scenario predictions). While the median expected ground motions for a CSZ rupture in Auburn, WA (~0.17 g) are anticipated to be less than the *PGA* for the SFZ scenarios (~0.27 g to 0.31 g), the larger magnitude Cascadia rupture (M_w9.0) would have a longer duration of shaking than a M_w7.2 SFZ rupture, thus leading to more cycles of loading and ultimately leading to similar liquefaction predictions in Auburn.

Bothell, Washington: Bothell, WA is approximately 20 km north of the SFZ. A majority of the SFZ liquefaction probabilities in Bothell are less than 5%, however, one study site has a probability over 50%. The *PGA*s at the study sites ~0.17 g to 0.25 g are certainly capable of triggering liquefaction, however, the soils at a majority of the study sites in Bothell are either not sufficiently loose, saturated, or cohesionless to liquefy, and/or the strata predicted to liquefy are interpreted to not be sufficiently thick or shallow to produce surface manifestations. In general, CSZ predictions are 0% to 20%, however, one study site exceeds 60% while a few others exceed 40%. Thus, the median probability of liquefaction predictions for a CSZ rupture are slightly larger than those of the SFZ scenarios in Bothell.

Issaquah, Washington: Issaquah, WA is approximately 20 km east of Seattle near the eastern extent of the SFZ. The liquefaction probabilities in Issaquah, WA generally range from 54% to 81%. The median CSZ liquefaction probabilities range from 33% to 72%, which are lower than the SFZ predictions although some locations still have relatively high probability.

Belfair, Washington: Belfair, WA is at the southwestern extent of the SFZ for all three scenarios near the terminus of the Hood Canal (fjord). The probability of manifestation near Belfair, WA was computed at a single study site and ranged from 69% for the northern scenario to 72% for the southern scenario. The median liquefaction prediction from a CSZ rupture was computed to be 75%, similar to the SFZ predictions.

While the SFZ scenario *PGA*s are 0.1 g to 0.2 g larger than the CSZ *PGA*, the increased duration of the CSZ earthquake causes the slightly larger liquefaction probability for this site.

Olympia, Washington: Olympia, WA is approximately 45 km south of the western end of the SFZ. The probabilities in Olympia, WA generally range from 15% to 60%. Compared to the median expected liquefaction impacts from a CSZ rupture, Rasanen et al. (2025) computed median liquefaction probabilities ranging from 40% to 90%, indicating liquefaction from a CSZ rupture is likely to be more prevalent compared to a SFZ rupture.

Seattle, Washington: All three SFZ scenarios traverse through the southern portion of Seattle and produce *PGA*'s generally ranging from ~0.5 g to 0.8 g in Seattle. Liquefaction probabilities over the portion of Seattle shown in Figure 3 are 62% on average, with 66% of sites having a probability greater than 60%. The northern scenario has a 5% larger liquefaction probability than the southern scenario on average. The median liquefaction probability for the 30 M_w9.0 CSZ simulations is on average 41% for the study sites within the extent shown in Figure 3. For these CSZ predictions, only 23% of study sites have a probability >60% given the smaller *PGA*s for the median CSZ rupture in general ranging from 0.10 g to 0.28 g. Therefore, while a CSZ earthquake is capable of being a M_w9.0, a M_w7.2 SFZ earthquake is anticipated to cause liquefaction impacts that would be far worse in Seattle compared to a CSZ earthquake due to Seattle residing so close to the SFZ and thus leading to high frequency ground motions 3-5 times larger than the high frequency motions from a CSZ earthquake. This does not mean all earthquake impacts in Seattle would be more severe for a SFZ rupture than a CSZ rupture. Surely, long period shaking and thus tall structures are more likely to be damaged from a CSZ earthquake given the low frequency motions generated by M_w9.0 subduction zone events. However, high frequency motions (e.g., *PGA*), which are best for predicting liquefaction (Sideras, 2019), are anticipated to be far more severe during a SFZ earthquake than the median expected liquefaction response of a CSZ earthquake. Even for the strongest expected shaking from a CSZ earthquake, which predicts 43% of study sites with a liquefaction probability exceeding 60% (Rasanen et al. 2025), the predicted impact remains substantially lower than that of the SFZ scenarios, where 66% of study sites shown in Figure 3 exceed the same liquefaction probability threshold.

In general, the liquefaction damage from a SFZ earthquake is anticipated to be worse than the median predictions from a CSZ earthquake in Seattle and along the I-5 corridor as far south as Auburn, WA to as far north as Bothell, WA. SFZ liquefaction predictions are expected to be worse east of Seattle as far as Issaquah, WA. Similar comparisons cannot be made west of I-5 due to the lack of high-quality data to predict liquefaction. One study site at the western extent of the SFZ near Belfair, WA had similar predictions between the SFZ scenarios and the median expected liquefaction response from a CSZ earthquake.

The higher predictions of liquefaction from a SFZ earthquake in the Seattle area may be preliminarily corroborated with paleoliquefaction evidence. Interestingly, at the time of writing this article, no liquefaction has been tied to the 1700 CSZ earthquake in the Puget Sound region, let alone any Cascadia Subduction Zone earthquake (Rasanen et al. 2023b; 2025), despite extensive searches (e.g., Atwater 1999; Bourgeois and Johnson 2001; Clague 2002; Clague et al. 1992, Clague et al. 1997, Davis 2018, Martin and Bourgeois 2012, Obermeier 1995; Rasanen et al. 2021). At the same time, liquefaction features constrained to about the time of the 923-924 CE SFZ earthquake have been found at several sites (Atwater 1999; Bourgeois and Johnson 2001; Whistler et al. 2002; Martin and Bourgeois 2012; Atwater personal communication 2020), including some liquefaction features (e.g., Bourgeois and Johnson 2001) extending up to a tsunami deposit tied to the 923-924 AD SFZ earthquake. This disparity between paleoliquefaction evidence for a SFZ versus CSZ earthquake suggests the SFZ poses a greater liquefaction hazard in Seattle and potentially other areas of the surrounding Puget Sound region.

3.3 Probability of Liquefaction-Induced Foundation Damage

The probabilities mapped in Figures 2 and 3 are those of surficial manifestations in the free field (i.e., liquefaction ejecta and/or ground cracking and deformation coinciding with potentially damaging instability). These manifestations strongly correlate with damage, particularly to shallow foundations, buried lifelines, pavements, and other near-surface infrastructure. However, liquefaction can potentially cause damage without otherwise expressing at the surface or can potentially express at the surface without causing damage. Asset-specific studies are therefore needed to predict the consequences of liquefaction more confidently. To that end, the 2010-2011 Canterbury, New Zealand, earthquakes resulted in unprecedented liquefaction case-history data (e.g., Geyin et al., 2021), including foundation damage surveys. To provisionally go beyond free-field manifestations and speculate on impacts, the foundation-damage models of Geyin et al. (2020b), which were trained using building performance data from Canterbury, were applied to the 268 study sites. These models are conditioned on the manifestation models adopted herein and are specific to 1-2 family residential structures on shallow foundations. The median probability of exceeding “moderate” foundation damage is mapped in Figure 4 for all three scenarios and in Figure 5 (Seattle extent) for the northern and southern SFZ scenarios. In this regard, the middle scenarios predictions fall between the north and south predictions and can be found mapped in supplemental Figure S.8. “Moderate” damage is defined as differential settlement more than 2 cm or global settlement exceeding 5 cm, but also includes five other modes of foundation deformation.

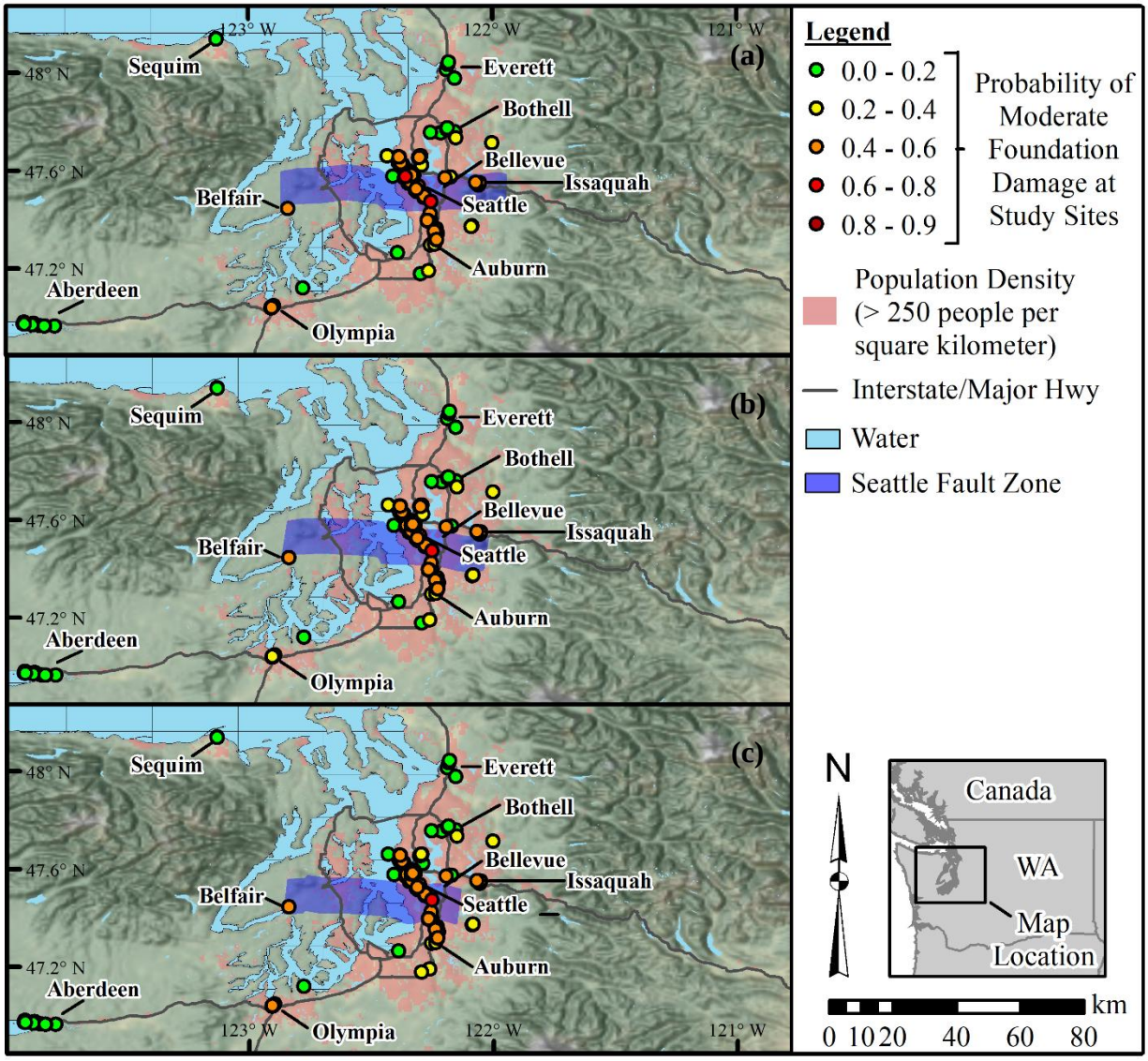

Fig. 4 Probability of moderate or greater foundation damage from liquefaction at 268 study sites considering the (a) northern; (b) middle; and (c) southern Seattle fault ground motion scenarios.

The median probability of such damage exceeds 40% at 69% of the study sites in Seattle, 88% of the sites in Auburn, 63% of the sites in Issaquah, and 15% of the sites in Olympia. As with the probabilities of free field manifestations, those of foundation damage also vary between the three SFZ scenarios by up to ~5%. Based on these preliminary analyses, damage to shallow foundations in Seattle and the surrounding suburbs like Auburn and Issaquah are likely to be relatively common for all scenarios whereas damage in locations like Olympia would likely be more sporadic.

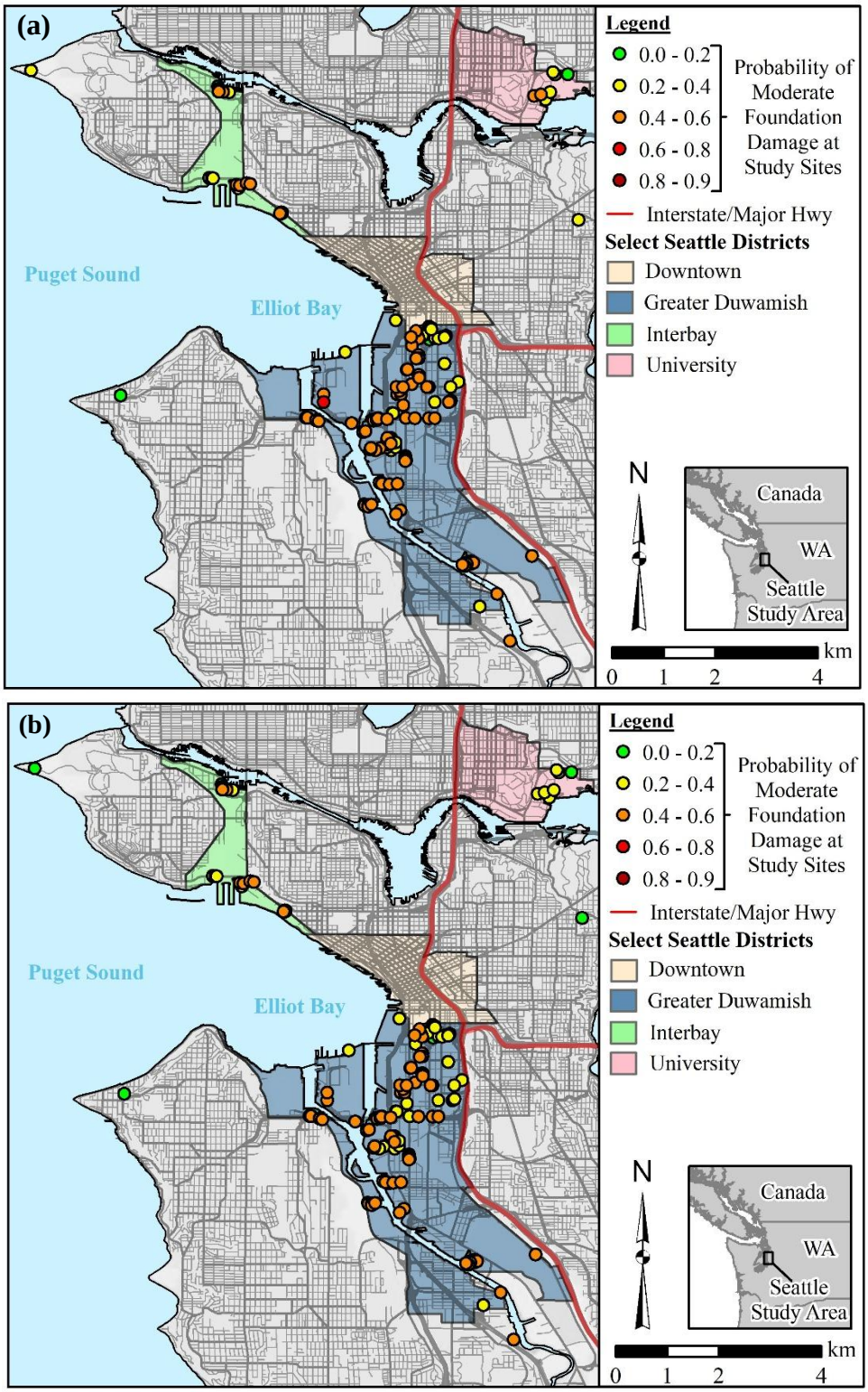

Fig. 5 Probability of moderate or greater foundation damage from liquefaction at 140 study sites in Seattle, WA, considering the (a) northern; and (b) southern SFZ ground motion scenarios.

These predictions do not account for potential, additional damage from: (i) lateral spreading, a particularly destructive effect of liquefaction influenced by local terrain; (ii) cyclic softening, which can induce permanent deformation in sensitive fine-grained materials; or (iii) seismic compression, which is the accrual of volumetric strains in dry or partially saturated soils that can lead to ground settlement during earthquake shaking, even at sites where the water table is too deep for damaging liquefaction. It is also important to recognize that: (i) shallow foundations supporting residential structures may not be present at the study sites, meaning these predictions are primarily illustrative; and (ii) many modern infrastructure assets (e.g., commercial, industrial, and large residential buildings) are constructed in compliance with building codes that mandate mitigation of liquefaction hazards, whether through ground improvement or more robust foundation systems. In contrast, older structures and other assets–-such as roads, utilities, and residential homes–-are less likely to have been designed with liquefaction considerations in mind. For example, single-family and duplex homes fall under the jurisdiction of the International Residential Code (e.g., IRC, 2021), which does not address liquefaction hazards, leaving mitigation up to individual homeowners and local officials. Given this regulatory gap, the low rate of earthquake insurance coverage in Washington—11.3% of residential homeowners are insured (Doughton and Gilbert 2018)—and the predictions mapped in Figures 4 and 5, liquefaction could pose a serious economic risk both to individual owners and to society at large. Ultimately, additional research is needed to predict the downstream consequences of liquefaction across the region.

3.4 Nuances, Uncertainties, and Further Discussion

The three M_w7.2 SFZ scenarios used in this study from the BSSC2014 scenario catalog are three interpretations of what a SFZ earthquake could look like. These scenarios originate from the 2008 National Seismic Hazard Map Update (Petersen et al. 2008) and model a M_w7.2 rupture on a thrust fault dipping at 45 degrees to the south with varying lengths and locations. Other moment magnitudes and fault geometries have been suggested. For example, Black et al. (2023) recently suggested the 923 to 924 AD SFZ rupture may have simultaneously ruptured with the Saddle Mountain fault located in the Olympia Peninsula and the energy released by this dual rupture was estimated at M_w7.8. Ultimately, as more SFZ paleoseismic evidence is discovered, dated, and inversed analyzed (e.g., Rasanen and Maurer 2022a,b,c; 2023) better ground motions estimates will arise. Furthermore, physics-based simulations such as Stone et al. (2022) and Frankel and Wirth et al. (2018) are becoming more prevalent and may provide better estimates of ground shaking intensity and uncertainty given they can account for complex effects such as topography and basins. Additionally, as for any liquefaction analysis, site response influences the ground motions. The site response used in this study used empirical site amplification factors based on V_{s30} (e.g., Seyhan and Stewart 2014). More sophisticated analyses such as non-linear site response analysis could be used instead.

Nonetheless, the predictions of liquefaction provided herein – based on a regional database of subsurface CPT data and an ensembling of 18 popular liquefaction models – are the most robust presently available.

4.0 Conclusion

This study provided a comprehensive forecast of regional liquefaction effects from three M_w7.2 SFZ earthquake scenarios by leveraging an ensemble of 18 popular CPT-based liquefaction models. These models were applied to 268 study sites of newly compiled subsurface geotechnical data across the Puget Sound region, resulting in 14,472 individual high-quality liquefaction predictions. Results for all three SFZ scenarios indicate that severe liquefaction is expected in Seattle, WA, and several nearby suburbs, particularly within 20 km of Seattle along the I-5 corridor, where fill and alluvial soils are prevalent. Comparisons with previous studies on the 2001 M_w6.8 Nisqually earthquake and a potential M_w9.0 Cascadia Subduction Zone rupture reveal that SFZ scenarios produce more severe liquefaction within ~20 km of Seattle due to higher shaking intensities at the study sites. Additionally, this study assessed the potential for liquefaction-induced shallow foundation damage. Damage is predicted to be relatively common in Seattle and surrounding suburbs, such as Auburn and Issaquah, but more sporadic in locations farther south, like Olympia. The extensive liquefaction and damage predictions made in this study may be useful to aid government agencies and stakeholders in preparing for future SFZ ruptures.

Statements and Declarations

Data Availability

Provided in a supplement is a GIS package containing the predicted probabilities of liquefaction manifestation and foundation damage at 268 study sites. A portion of the CPT data used in this study was funded by the U.S. Geological Survey and are available in Grant et al. (2024). Numerous additional CPTs used were compiled from various partners and sources and are available in Rasanen et al. (2024).

Funding

No funds, grants, or other support were received during the preparation of this manuscript.

Competing Interests

The authors have no relevant financial or non-financial interests to disclose.

References

Architectural Institute of Japan (2001) *Recommendations for design of building foundations*, 486 p.

Allstadt, K., J. E. Vidale, and A. D. Frankel (2013) A scenario study of seismically induced landsliding in Seattle using broadband synthetic seismograms, *Bull. Seismol. Soc. Am.* 103, no. 6, 2971–2992.

Atwater, B.F. (1999). "Radiocarbon dating of a Seattle earthquake to A.D. 900–930." *SRL* 70: 232.

Atwater, B.F., and A.L. Moore (1992) A tsunami about 1000 years ago in Puget Sound, Washington, *Science* 258, no. 5088, 1614–1617.

Black, B. A., J. K. Pearl, C. L. Pearson, P. T. Pringle, D. C. Frank, M. T. Page, B. M. Buckley, E. R. Cook, G. L. Harley, K. J. Heeter, et al. (2023) A multi-fault earthquake threat for the Seattle metropolitan region revealed by mass tree mortality, Sci. Adv. 9, no. 39, eadh4973, doi: 10.1126/sciadv.adh4973.

Boulanger, R.W. and Idriss, I.M. (2006) Liquefaction susceptibility criteria for silts and clays. *Journal of Geotechnical and Geoenvironmental Engineering* 132(11): 1413-1426.

Boulanger RW and Idriss IM (2016) CPT-based liquefaction triggering procedure. *Journal of Geotechnical and Geoenvironmental Engineering* 142(2): 04015065.

Bourgeois, J., and Johnson, S.Y. (2001). Geologic evidence of earthquakes at the Snohomish delta, Washington, in the past 1200 yr. *Geological Society of America Bulletin* 113(4): 482-494.

Bray JD, Sancio R, Kammerer AM, Merry S, Rodriguez-Marek A, Khazai B, ... and Nykamp M (2001) *Some observations of the geotechnical aspects of the February 28, 2001, Nisqually earthquake in Olympia, South Seattle, and Tacoma, Washington*. Report sponsored by NSF, PEER, UCB, University of Arizona, Washington State University, Shannon and Wilson Inc., and Leighton and Associates.

Bucknam, R.C., Hemphill-Haley, E. and Leopold, E.B. (1992) Abrupt uplift within the past 1700 years at southern Puget Sound, Washington. *Science*, 258, 1611–1614.

Chamberlin C., and Arcas D. (2015) Modeling tsunami inundation for hazard mapping at Everett, Washington, from the Seattle Fault." NOAA Technical Memorandum OAR PMEL-147, http://doi.org/10.7289/V59Z92V0.

Chiou B.S.-J., and Youngs R.R. (2014) Update of the Chiou and Youngs NGA Model for the Average Horizontal Component of Peak Ground Motion and Response Spectra. *Earthquake Spectra* 30 (3): 1117–1153. doi: https://doi.org/10.1193/072813EQS219M

Chleborad AF and Schuster RL (1990) Ground failure associated with the Puget Sound region earthquakes of April 13, 1949 and April 29, 1965. United States Geological Survey Open-File Rept.

Chin, T., and Evans, T.M. (2021) GOSEP: Georeferenced Oregon Soil Engineering Properties. Ver. 2.0, Accessed from http://ohelp.oregonstate.edu/GOSEP/user_manual.pdf on 6 June 2023.

Clague, J. J. (2002). The earthquake threat in southwestern British Columbia: A geologic perspective. *Natural Hazards*, *26*, 7-33.

Clague, J.J., Naesgaard, E., and Nelson, A.R. (1997) Age and significance of earthquake-induced liquefaction near Vancouver, British Columbia, Canada. *Can. Geotech. J.* 34: 53-62.

Clague, J.J., Naesgaard, E., and Sy, A. (1992) Liquefaction features on the Fraser delta: evidence for prehistoric earthquakes? *Canadian Journal of Earth Sciences* 29: 1734.1745.

Creager, K., Crosson, R., Pratt, T., Weaver, C., Kramer, S., MacRae, G., ... & Chang, S. (2001) The Nisqually Earthquake of 28 February 2001 Preliminary Reconnaissance Report. *Nisqually Earthquake Clearinghouse Group, University of Washington Seattle, WA*.

Davis E. (2018) Evidence for liquefaction and flooding in the past 1,000 years along the Duwamish River, Seattle, Washington. M.S. thesis, University of Washington.

de Magistris, F.S., Lanzano, G., Forte, G., Fabbrocino, G. (2013) A database for PGA threshold in liquefaction occurrence. Soil Dyn. Earthq. Eng. 54, 17–19.

Dolcimascolo, Alexander; Eungard, D. W.; Allen, Corina; LeVeque, R. J.; Adams, L. M.; Arcas, Diego; Titov, V. V.; González, F. I.; Moore, Christopher (2022) Tsunami inundation, current speeds, and arrival times simulated from a large Seattle Fault earthquake scenario for Puget Sound and other parts of the Salish Sea: Washington Geological Survey Map Series 2022-03, 16 sheets, scale 1:48,000, 51 p. text. https://fortress.wa.gov/dnr/geologydata/tsunami_hazard_maps/ger_ms2022-03_tsunami_hazard_seattle_fault.zip

Doughton and Gilbert (2018) Survey finds only 11.3% of Washington homes have earthquake insurance. *Seattle Times*, February 7, 2018. Accessed from < https://shorturl.at/aqxE6> 1 June 2023.

FEMA (2019) Hazus Earthquake Model Technical Manual. Federal Emergency Management Agency, Washington D.C.

Frankel, A., Wirth, E., Marafi, N., Vidale, J., and Stephenson, W. (2018) Broadband Synthetic Seismograms for Magnitude 9 Earthquakes on the Cascadia Megathrust Based On 3D Simulations and Stochastic Synthetics (Part 1): Methodology and Overall Results. *BSSA* 108 (5A): 2347-2369.

Geyin, M. and Maurer, B.W. (2021a) Fragility functions for liquefaction induced ground failure. *Journal of Geotechnical and Geoenvironmental Engineering,* 146(12): 04020142.

Geyin, M. and Maurer, B. W. (2021b) Evaluation of a cone penetration test thin-layer correction procedure in the context of global liquefaction model performance. *Engineering Geology, 291*, 106221.

Geyin, M., Baird, A. J., & Maurer, B.W. (2020a) Field assessment of liquefaction prediction models based on geotechnical versus geospatial data, with lessons for each. *Earthquake Spectra*, *36*(3), 1386-1411.

Geyin, M., Maurer, B. W., & van Ballegooy, S. (2020b) Lifecycle Liquefaction Hazard Assessment and Mitigation. In *Geo-Congress 2020: Biogeotechnics* (pp. 312-320). Reston, VA: ASCE.

Geyin, M., Maurer, B. W., Bradley, B. A., Green, R. A., & van Ballegooy, S. (2021) CPT-based liquefaction case histories compiled from three earthquakes in Canterbury, New Zealand. *Earthquake Spectra*, *37*(4), 2920-2945.

Grant, W.P., (1986) The potential for ground failures in the Puget Sound area, *in* Hays, W.W., and Gori, P.L., eds., Proceedings of Conference XXXIII, Workshop on earthquake hazards in the Puget Sound, Washington, area: U.S. Geological Survey Open-File Report 86–253, p. 134–138.———1990, Evaluation of liquefaction potential, Seattle, Washington: U.S. Geological Survey report, Contract no. 14–08–0001–G–1385, 47 p.

Grant A. (2017) *Regional-scale coseismic landslide hazard modeling and consequence analysis*. PhD Dissertation, University of Washington, Seattle, WA

Grant, A.R.R., Svitek, J.F., Rasanen, R.A., Maurer, B.W., and Greenfield, M.W. (2024) Cone Penetration Test data of Paleoliquefaction sites in Washington and Oregon: U.S. Geological Survey data release, https://doi.org/10.5066/P9XMD80B.

Green, R. A., J. J. Bommer, A. Rodriguez-Marek, B. W. Maurer, P. J. Stafford, B. Edwards, P. P. Kruiver, G. De Lange, and J. Van Elk (2019) Addressing limitations in existing 'simplified' liquefaction triggering evaluation procedures: application to induced seismicity in the Groningen gas field. *Bulletin of Earthquake Engineering* 17(8), 4539-4557.

Herzig E., Duvall A., Booth A., Stone I., Wirth E., LaHusen S., Wartman J., and Grant A. (2024) Evidence of Seattle Fault Earthquakes from Patterns in Deep-Seated Landslides. *Bull. Seismol. Soc. Am.* 114, 1084-1102, doi: 10.1785/0120230079.

Huang, Y., Yu, M. (2013) Review of soil liquefaction characteristics during major earthquakes of the twenty-first century. *Natural Hazards* **65**, 2375–2384, https://doi.org/10.1007/s11069-012-0433-9

Idriss, I.M., and Boulanger, R.W. (2008) Soil liquefaction during earthquakes. *Monograph MNO-12* 2008; Earthquake Engineering Research Institute, Oakland, CA, 261 pp.

International Residential Code (IRC) (2021). International Code Council. ISBN 978-1-60983-957-4.

Iwasaki, T, Tatsuoka, F, Tokida, K, and Yasuda, S.A. (1978) Practical method for assessing soil liquefaction potential based on case studies at various sites in Japan. *2nd Int. Conf. on Microzonation*, San Francisco, USA.

Jacoby, G. C., P. L. Williams, and B. M. Buckley (1992) Tree ring correlation between prehistoric landslides and abrupt tectonic events in Seattle, Washington, Science 258, no. 5088, 1621–1623.

Jeschke, D.A., Eungard, D.W., Troost, K.G., Wisher, A.P, (2019) Subsurface database of Washington State - GIS data. Washington Geological Survey Digital Data Series 11, version 2.1, previously released August 2017, Accessed from https://geologyportal.dnr.wa.gov/ on 6 June 2023.

Karlin, R. E., M. Holmes, S. E. B. Abella, and R. Sylwester (2004) Holocene landslides and a 3500-year record of Pacific Northwest earthquakes from sediments in Lake Washington, GSA Bull. 116, nos. 1/2, 94–108.

Koshimura, S., Katada, T., Mofjeld, H.O. *et al.* (2006) A method for estimating casualties due to the tsunami inundation flow. *Natural Hazards* **39**, 265–274, https://doi.org/10.1007/s11069-006-0027-5

Liberty, L.M., and Pratt, T.L. (2008) Structure of the eastern Seattle fault zone, Washington State: New insights from seismic reflection data: *Seismological Society of America Bulletin*, v. 98, p. 1681–1695, doi:10.1785/0120070145.

Ludwin, R. S., C. P. Thrush, K. James, D. Buerge, C. Jonientz-Trisler, J. Rasmussen, K. Troost, and A. De Los Angeles (2005). Serpent spirit-power stories along the Seattle fault, Seismol. Res. Lett. 76, no. 4, 426–431.

Martin, M.E. (2012) The A.D. 900–930 Seattle-Fault-Zone Earthquake with a Wider Coseismic Rupture Patch and Postseismic Submergence: Inferences from New Sedimentary Evidence *Bulletin of the Seismological Society of America*, Vol. 102, No. 3, pp. 1079–1098, June 2012, doi: 10.1785/0120110123

Martin, M.A., and Bourgeois, J. (2012) Vented sediments and tsunami deposits in the Puget Lowland, Washington – differentiating sedimentary processes. *Sedimentology* 59: 419-444.

Maurer, B.W., Green, R.A. and Taylor, O.D.S. (2015) Moving towards an improved index for assessing liquefaction hazard: lessons from historical data. *Soils and Foundations* 55(4): 778-787.

Maurer, B.W., Green, R.A., van Ballegooy, S. and Wotherspoon, L. (2019) Development of region-specific soil behavior type index correlations for evaluating liquefaction hazard in Christchurch, New Zealand. *Soil Dynamics and Earthquake Engineering* 117: 96-105.

Moss R.E.S., Seed R.B., Kayen R.E., Stewart J.P., Der Kiureghian A., Cetin K.O. (2006) CPT-based probabilistic and deterministic assessment of in situ seismic soil liquefaction potential. *Journal of Geotechnical and Geoenvironmental Engineering*, 132(8), 1032-1051.

Nelson, A. R., S. F. Personius, B. L. Sherrod, H. M. Kelsey, S. Y. Johnson, L. A. Bradley, and R. E. Wells (2014) Diverse rupture modes for surface-deforming upper plate earthquakes in the southern Puget Lowland of Washington State, Geosphere 10, no. 4, 769–796.

Obermeier, S. F. (1995) Preliminary estimates of the strength of prehistoric shaking in the Columbia River Valley and the southern half of coastal Washington, with emphasis for a Cascadia Subduction Zone earthquake about 300 years ago. *U.S. Geol. Surv.* Open-File Rept. 94-589, 46 pp.

Parker, M and Steenkamp, D. (2012) The economic impact of the Canterbury earthquakes. Bulletin of the *Reserve Bank of New Zealand:* 75(3): 13–25.

Petersen, M. D., Frankel, A. D., Harmsen, S. C., Mueller, C. S., Haller, K. M., Wheeler, R. L., ... & Rukstales, K. S. (2008) *Documentation for the 2008 update of the United States national seismic hazard maps* (No. 2008-1128). US Geological Survey.

Petersen, M. D., Moschetti, M.P., Powers, M.P., Mueller, C.S., Haller, K.M., Frankel, A.D., … & Olsen, A.H. (2014) *Documentation for the 2014 update of the United States national seismic hazard maps* (No. 2014-1091). U.S. Geological Survey.

Rasanen, R. A., Marafi, N. A., & Maurer, B. W. (2021) Compilation and forecasting of paleoliquefaction evidence for the strength of ground motions in the US Pacific Northwest. *Engineering Geology*, *292*, 106253. https://doi.org/10.1016/j.enggeo.2021.106253.

Rasanen, R. A., & Maurer, B. W. (2022a) Seismic Source Parameters from Regional Paleoseismic Evidence. In *Geo-Congress 2022* (pp. 411-420). https://doi.org/10.1061/9780784484043.040.

Rasanen, R. A., & Maurer, B. W. (2022b). Probabilistic seismic source location and magnitude via inverse analysis of paleoliquefaction evidence. *Earthquake Spectra*, *38*(2), 1499-1528. https://doi.org/10.1177/87552930211056355.

Rasanen, R.A., Maurer, B.W. (2022c) "Probabilistic seismic source inversion from regional landslide evidence." *Landslides* 19, 407–419. https://doi.org/10.1007/s10346-021-01780-9

Rasanen, R. A., & Maurer, B. W. (2023) Probabilistic seismic source inversion of the 1886 Charleston, South Carolina, earthquake from macroseismic evidence: A major updating. *Engineering Geology*, 312, 106958. https://doi.org/10.1016/j.enggeo.2022.106958.

Rasanen, R.A., Geyin, M., and Maurer, B.W. (2023a) Select Liquefaction Case Histories from the 2001 Nisqually, Washington Earthquake: A Digital Dataset and Assessment of Model Performance. *Earthquake Spectra*. https://doi.org/10.1177/87552930231174244.

Rasanen, R.A., Wood, C.M., and Maurer, B.W. (2023b) Constraining Cascadia Subduction Zone Ground Motions via Paleoliquefaction Evidence: A Case Study from Kellogg Island, Washington, with Regional

Implications. In: *Proceedings of GeoCongress 2024* (pp. 141-151). https://doi.org/10.1061/9780784485316.016.
Rasanen, R., M. Geyin, M. Sanger, B. Maurer. (2024) A Database of Cone Penetration Tests from the Cascadia Subduction Zone. DesignSafe-CI. https://doi.org/10.17603/ds2-snvw-jv27 v1
Rasanen, R.A., Grant, A., Makdisi, A.J., Maurer, B.W., Wirth, E. (2025) Implications of Physics-Based M9 Ground Motions on Liquefaction-Induced Damage in the Cascadia Subduction Zone: Looking Forward and Backward. *Earthquake Spectra*.
Raulerson, A.A. (2021) Tsunami Deposits and Tsunami Modeling of the 900 AD Seattle Fault Event in Northern Puget Sound. All Master's Theses. 1551. https://digitalcommons.cwu.edu/etd/1551
Robertson, P.K., and Wride, C.E. (1998) Evaluating cyclic liquefaction potential using cone penetration test. *Canadian Geotechnical Journal*, 35(3), 442-459.
Rogers A.M., Walsh T.J., Kockelman W.J., Priest G.R. (1998) Assessing Earthquake Hazards and Reducing Risk in the Pacific Northwest. *U.S. Geological Survey Paper 1560*.
Schuster, R. L., R. L. Logan, and P. T. Pringle (1992) Prehistoric rock avalanches in the Olympic Mountains, Washington, Science 258, no. 5088, 1620–1621.
Seed, H.B. & Idriss, I.M. (1971) Simplified procedure for evaluating soil liquefaction potential, *ASCE Journal of Soil Mechanics and Foundations Division* 97(9), 1249–1273.
Seyhan E, and Stewart JP (2014) Semi-Empirical Nonlinear Site Amplification from NGA-West2 Data and Simulations. *Earthquake Spectra* 30(3):1241-1256. doi:10.1193/063013EQS181M
Sherrod, B.L. (2001) Evidence for earthquake induced subsidence about 1100 yr ago in coastal marshes of southern Puget Sound, Washington. *Geological Society of America Bulletin*, v. 113, p. 1299–1311.
Sideras, S. (2019). *Evolutionary intensity measures for more accurate and informative evaluation of liquefaction triggering.* PhD Dissertation, University of Washington, Seattle, WA.
Stewart, M. (2005). Scenario for a magnitude 6.7 earthquake on the Seattle Fault. Earthquake Engineering Institute and Washington Military Department, Emergency Management Division, 162 pp.
Stone, I., E. A. Wirth, and A. D. Frankel (2022) Topographic response to simulated M w 6.5–7.0 earthquakes on the Seattle fault, *Bull. Seismol. Soc. Am.* 112, no. 3, 1436–1462.
Styron, R. H., and B. Sherrod (2021). Improving paleoseismic earthquake magnitude estimates with rupture length information: Application to the Puget Lowland, Washington State, USA, *Bull. Seismol. Soc. Am.* 111, no. 2, 1139–1153.
ten Brink, U. S., J. Song, and R. C. Bucknam (2006) Rupture models for the AD 900–930 Seattle fault earthquake from uplifted shorelines, Geology 34, no. 7, 585–588.
Thompson, E. M., Wald, D. J., Worden, B., Field, N., Luco, N., Petersen, M. D., ... & Badie, R. (2016). *Shakemap earthquake scenario: building seismic safety council 2014 event set (BSSC2014)*. Technical report, US Geological Survey Digital Object Identifier Catalog.
Van Ballegooy, S., Malan, P., Lacrosse, V., Jacka, M.E., Cubrinovski, M., Bray, J.D., O'Rourke, T.D., Crawford, S.A., and Cowan, H. (2014) Assessment of liquefaction-induced land damage for residential Christchurch. *Earthquake Spectra*, 30(1): 31-55.
Whistler, J.E., Atwater, B.F. and Montgomery, D.R. (2002) Holocene liquefaction near the Seattle fault at the Issaquah Creek delta. *Eos*, 83, S22B–1036.
Wirth, E. A., Frankel, A. D., Marafi, N., Vidale, J. E., and Stephenson, W. J. (2018) Broadband Synthetic Seismograms for Magnitude 9 Earthquakes on the Cascadia Megathrust based on 3-D Simulations and Stochastic Synthetics (Part 2): Rupture Parameters and Variability. *BSSA*, 108 (5A): 2370-2388.
Worden, B.C. and Heath, D.C. (2019). Global VS30 Map. GitHub, https://github.com/usgs/earthquake-global_vs30.
WSDOT (2021) Geotech Data Historic Borings. Washington State Department of Transportation (WSDOT), WSDOT Online Map Center. Accessed from https://geo.wa.gov/ on 6 June 2023.
Yost, K. M., Green, R. A., Upadhyaya, S., Maurer, B. W., Yerro-Colom, A., Martin, E. R., & Cooper, J. (2021) Assessment of the efficacies of correction procedures for multiple thin layer effects on Cone Penetration Tests. *Soil Dynamics and Earthquake Engineering*, *144*, 106677.